X-Ray Emission during the Muonic Cascade in Hydrogen

B. Lauss,* P. Ackerbauer, W. H. Breunlich, B. Gartner, M. Jeitler, P. Kammel,† J. Marton, W. Prymas, and J. Zmeskal
Institute for Medium Energy Physics, Austrian Academy of Sciences, Boltzmanngasse 3, A-1090 Wien, Austria

D. Chatellard, J.-P. Egger, and E. Jeannet
Institut de Physique de l'Université, CH-2000 Neuchâtel, Switzerland

H. Daniel, F. J. Hartmann, and A. Kosak
Physics Department, TU München, D-8574 Garching, Germany

C. Petitjean
Paul Scherrer Institut, CH-523 Villigen, Switzerland
(Received 12 September 1997)

We report our investigations of x rays emitted during the muonic cascade in hydrogen employing charge coupled devices as x-ray detectors. The density dependence of the relative x-ray yields for the muonic hydrogen lines (K_α, K_β, and K_γ) has been measured at densities between 0.001 15 and 0.97 of liquid hydrogen density. In this density region collisional processes dominate the cascade down to low energy levels. A comparison with recent calculations is given in order to demonstrate the influence of Coulomb deexcitation. [S0031-9007(98)05692-0]

PACS numbers: 36.10.Dr, 32.30.Rj, 32.70.Fw

Exotic atoms are atoms in which an electron is replaced by a heavier negatively charged particle, e.g., $\mu^-, \pi^-, K^-, \overline{p}$. The simplest of these atoms is muonic hydrogen μp, which denotes a bound state of one proton and one muon.

After a free muon is injected into a hydrogen target, it is slowed down, and an excited muonic hydrogen atom is formed via Coulomb capture [1,2], leaving the muon most likely in an initial state of $11 \leq n \leq 15$ [3]. This is the starting point for a complicated interplay of competitive collisional and radiative deexcitation processes, the so-called atomic cascade, which ends with the muonic atom being in the $1s$ ground state. The possibility of a metastable $2s$ state in muonic hydrogen is currently under investigation [4].

Muons, in contrast to the other possible particles, are not affected by strong interaction. So they may serve as the best probe for the investigation of these deexcitation processes.

At the investigated hydrogen densities, collisional deexcitation dominates from the beginning of the cascade to low n states, depending on the target density and the kinetic energy of the μp atom [1,5–8]. The known collisional processes are chemical dissociation, elastic collision, external Auger electron emission, Coulomb deexcitation, and Stark mixing. The importance of the last two effects is due to the very small size of the neutral μp atom, which can penetrate very deeply into the electron cloud of a neighboring H_2 molecule, where it can "feel" the electromagnetic field of the protons.

In the investigated hydrogen gases, the transitions to the ground state are always accompanied by the emission of muonic x rays; at liquid hydrogen density (LHD) [9], the x-ray emission probability is still 0.95 [7].

All these processes together make up the "standard cascade model" [1,5,6,10,11] which, despite its success, has one severe limitation: this is the assumption that $\epsilon_{\mu p}$, the kinetic energy of the μp atom, is constant throughout the cascade.

A recent calculation [7,8] tries to take into account the time evolution of $\epsilon_{\mu p}$ for energy levels $n \leq 6$. Because of Coulomb deexcitation, complex energy distributions at various levels are expected. Coulomb deexcitation is the only known mechanism which can accelerate μp atoms up to epithermal energies of $\sim$170 eV [7]. In spite of its importance, Coulomb deexcitation is regarded as the least known process of the muonic cascade (neglecting chemical deexcitation, which is important only at very high energy levels) [8]. Existing calculations of the Coulomb deexcitation cross sections differ among themselves by more than 1 order of magnitude [12–16].

Apart from the basic interest in exotic atoms, the understanding of the deexcitation of muonic atoms is of great importance for various other phenomena, such as muon catalyzed fusion [17–19], muon transfer [20–22], diffusion of muonic atoms [23], and nuclear muon capture [24,25]. The muonic case can also be used as a test for the cascade in hadronic atoms [26] (e.g., $\pi^- p$) where velocity effects [27,28] severely affect the evaluation of strong interaction parameters [29,30].

For this measurement, the relative x-ray yields of the emitted muonic hydrogen $K^{\mu p}$ lines—the corresponding x-ray energies are $K_\alpha = 1.90$ keV, $K_\beta = 2.25$ keV, $K_\gamma = 2.37$ keV, and $K_\infty = 2.53$ keV—and their intensity ratios serve as a tool to investigate the muonic cascade.

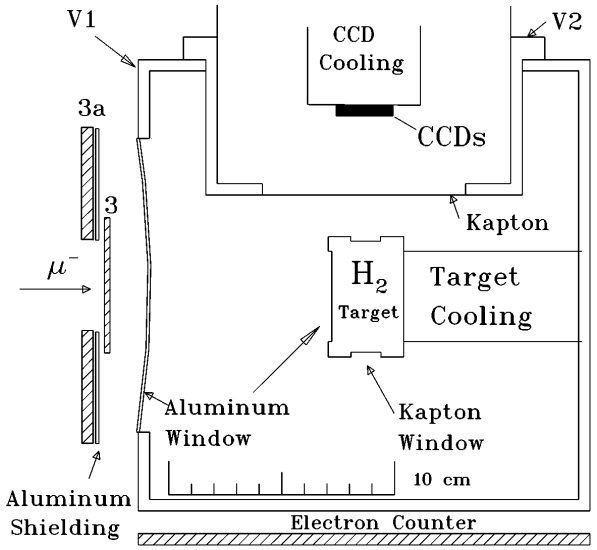

FIG. 1. Top view of the setup of this experiment. The displayed target cell was used for the measurements in liquid hydrogen. Two separated vacuum vessels were used; one for the target (V1), and one for the CCD detector (V2). To ensure an optimal stopping efficiency the scintillation counters 3 and 3a were used to register incoming muons. The electron counter served to detect muon decay electrons. Larger target cells, adapted to the expected extent of the muon stopping distributions, were used for the measurements in gaseous hydrogen [36].

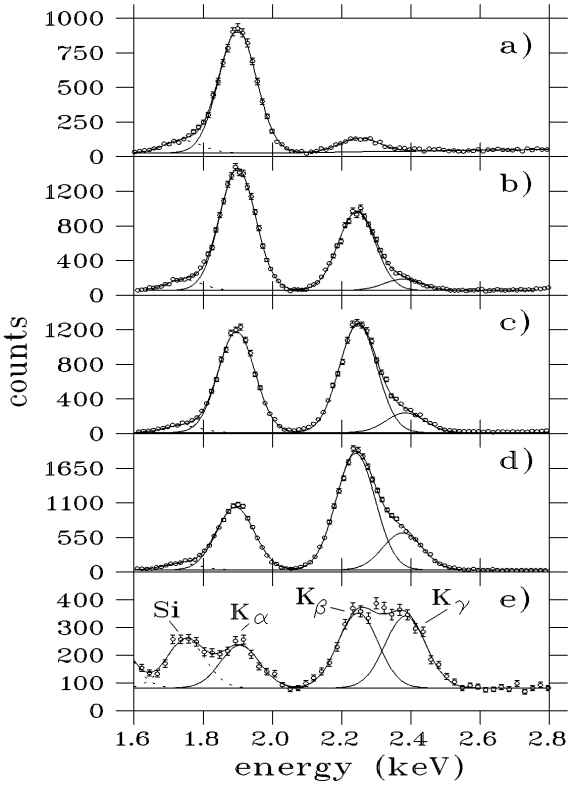

FIG. 2. Muonic x-ray energy spectra in hydrogen observed with a CCD detector at temperatures of ~30 K and various target densities Φ (given in units of LHD): (a) $\Phi = 0.97$; (b) $\Phi = 0.0795$; (c) $\Phi = 0.0391$; (d) $\Phi = 0.0106$; and (e) $\Phi = 0.001\,15$. K_α, K_β, and K_γ lines could be separated. The energy resolution of the detector $\Delta E^{\mathrm{FWHM}}/E$ at 2 keV was 6%. The solid lines indicate Gaussian fits. The density dependence of the line intensities is clearly visible. The x-ray peak at 1.74 keV (dashed line) is due to fluorescence excitation of the detector's silicon material. The low counting statistics and the high background Si peak visible in measurement (e) reflects the already very low stopping probability of muons in such a low-density hydrogen gas.

This is the first systematic investigation of muonic x rays in this density region, and the first one which gives intensities for the three lowest muonic K lines. Earlier experiments [31–35] were either rather inaccurate or performed at very low gas densities ($<10^{-3} \times$ LHD) only.

Our measurements were carried out with the high intensity muon beam of the $\mu E4$ area at PSI (Paul Scherrer Institut, Villigen, Switzerland). Figure 1 shows the setup for the measurements at liquid hydrogen density. Several different silver-coated steel or aluminum target cells were optimized for the measurements in liquid and gaseous hydrogen, respectively [36].

To minimize x-ray absorption, Kapton windows with a thickness of 12.5 μm were used for the measurements at LHD. The gas target equipped with 25 μm thick windows had to withstand pressures of up to 6 bar at temperatures around 30 K. For safety reasons, the target vacuum vessel was separated from the vacuum of the charge coupled device (CCD) with an additional 12.5 μm Kapton window. The target cells were partly covered with superinsulation to reduce radiation heating.

To avoid high Z impurities in the target, which would change the K line intensities through excited-state muon transfer [20,37], the hydrogen was cleaned during the filling procedure by using a liquid-nitrogen trap together with a palladium filter. Wall effects were calculated to be negligible, and this was confirmed by a monitoring diode detector to an accuracy better than 0.1%. The composition of the hydrogen was checked on-line during the measurements by using a quadrupole mass spectrometer [38] which could extract samples via a small capillary leading directly into the target volume. The stability of the target pressure and temperature was monitored and controlled during all measurements.

Charge coupled devices [39,40] have been employed as x-ray detectors. They consisted of two CCD sensors [41] with an active detection area of $\sim 25 \times 17$ mm^2 (~880 000 pixels) for each chip. The main chip component was silicon with small absorption layers of SiO_2 and Si_3N_4 on the surface. The depletion thickness of ~30 μm was well adapted for the observed energy region. To shorten the readout time, each chip was split into two electronically independent detection areas.

We were able to apply a specific pattern recognition algorithm to separate "true" x-ray hits from charged particles and cosmic background using a "single pixel" selection criterion [42–44]. A single pixel was considered to be a true x ray if the charge content of the surrounding

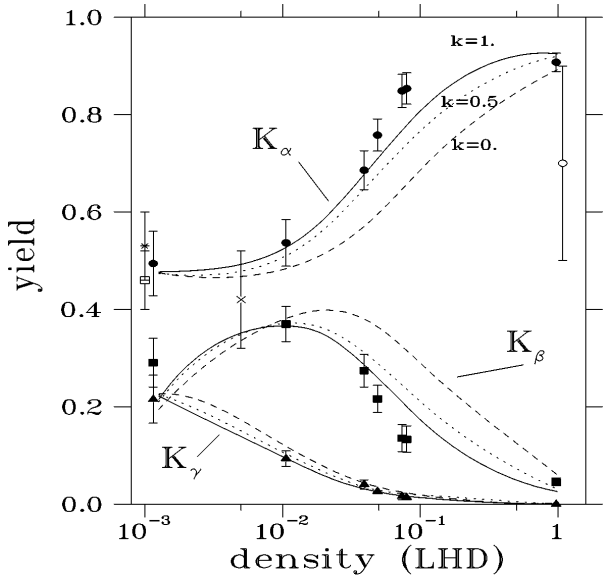

FIG. 3. The density dependence of the yield of muonic K lines in hydrogen. The measured relative yield is given as the number of counts in one K line ($K_i, i = \alpha, \beta, \gamma$) divided by the total count rate in all observed K lines ($K_{\text{tot}} = K_\alpha + K_\beta + K_\gamma$). The plotted data points at LHD include a 5% correction for nonradiative ground state transitions [7]. Filled circles, squares, and triangles indicate the relative yield for K_α, K_β, and K_γ transitions, respectively. The other experimental points for K_α yields are taken from Refs. [31] (cross), [32] (open circle), [33] (star), and [34] (square). The displayed calculated results from [8] used a scaling factor k for the Coulomb deexcitation cross section; $k = 0$ (dashed line), $k = 0.5$ (dotted line), and $k = 1$ (full line).

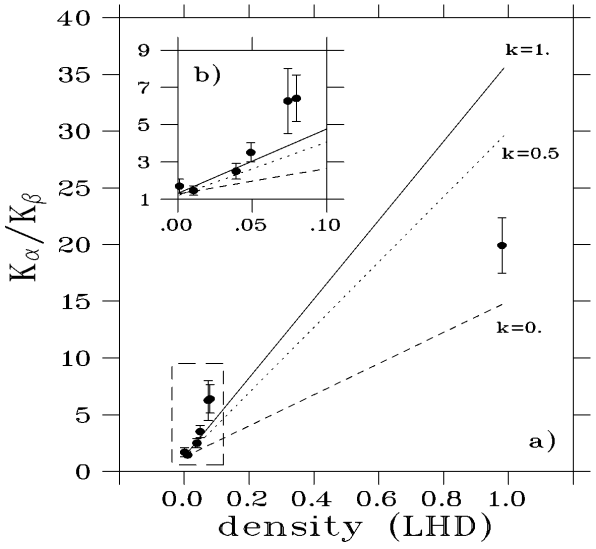

FIG. 4. (a) The density dependence of the K_α/K_β ratio in muonic hydrogen. The theoretical curves are calculated as in Fig. 3. The inset (b) displays the magnified low density region.

eight neighbor pixels was statistically compatible with the noise peak of the CCDs.

Data runs lasted for ~3 min to guarantee that not more than ~15% of the CCD's pixels were hit. A longer exposure time would have caused a decrease in the detection efficiency. A fraction of hit pixels of more than 40% actually would have made it very difficult to apply our selection criterion for x rays.

Our measurements investigated a density region covering 3 orders of magnitude. The observed raw energy spectra are displayed in Fig. 2. The intensity variation of the muonic hydrogen K_α, K_β, and K_γ lines with target density can be seen directly. No K lines higher than K_γ could be observed.

An empty target run and a μ^+ run proved that there were no background peaks visible within the relevant energy region. The x-ray peak at 1.74 keV is due to fluorescence excitation of the detector's silicon material. Therefore the background function could be approximated by the sum of a constant and a term depending linearly on energy. Gaussians with energy-dependent width [36,42] were used to fit the peak areas of muonic hydrogen and of silicon.

The knowledge of the x-ray detection efficiency was indispensable for a correct analysis. A Monte Carlo program was written [36] to correctly account for the various contributions to x-ray absorption. The geometry of the different target cells, the absorption in the windows and in the CCDs' top layers was simulated. The intrinsic detection efficiency of the CCDs was checked at the ~10% level using the known intensity ratios of antiprotonic x rays. The absorption in the window foils was measured with an ^{55}Fe source and various material layers [36].

Figure 3 displays our results, given in Table I for the x-ray yields of the muonic hydrogen $2 \rightarrow 1$, $3 \rightarrow 1$, and $4 \rightarrow 1$ transitions. The relative yield is given by the intensity of one specific K line ($K_i, i = \alpha, \beta, \gamma$) divided by the intensity of all observed K lines ($K_{\text{tot}} = \sum_i K_i$). For all gas points, the measured relative yield is equivalent to the calculated yield; at LHD, a 5% correction for nonradiative ground state transfer has to be applied [7] for comparison with theory. This is the first measurement which allows us to test the existing cascade calculations at high target densities [5,7,8,10]. The calculations taken from [8] shown in Figs. 3 and 4 were done for different contributions of Coulomb deexcitation. There, the corresponding cross sections [12] were scaled with a factor $k = 0$ (no contribution, dashed line), $k = 0.5$ (dotted line), and $k = 1$ (full line). The calculation according to the standard cascade model [5,10] coincides with the $k = 0$ assumption. The displayed data—error bars include statistical errors and contributions due to efficiency corrections—match quite well the calculated density dependence. Though not very sensitive to k within the experimental errors, the yield measurements favor values of $k \sim 1$.

Theory [8] predicts that in the observed density region the density dependence of the K_α/K_β ratio is approximately linear, with a significant contribution from Coulomb deexcitation. Figure 4 shows our results (Table I) together with the calculation from [8]. The K_α/K_β value at LHD favors a scaling factor $k < 0.5$.

TABLE I. Results of the muonic x-ray measurements in hydrogen.

Density [LHD]	K_α/K_{tot}	K_β/K_{tot}	K_γ/K_{tot}	K_α/K_β
0.9700 ± 0.0030	0.952 ± 0.019	0.048 ± 0.008	0.000 ± 0.010	19.9 ± 2.45
0.0795 ± 0.0008	0.854 ± 0.032	0.133 ± 0.027	0.013 ± 0.006	6.41 ± 1.25
0.0738 ± 0.0008	0.849 ± 0.034	0.135 ± 0.028	0.016 ± 0.007	6.27 ± 1.75
0.0489 ± 0.0004	0.758 ± 0.033	0.216 ± 0.028	0.026 ± 0.007	3.51 ± 0.52
0.0391 ± 0.0003	0.686 ± 0.040	0.274 ± 0.034	0.040 ± 0.009	2.50 ± 0.42
0.0106 ± 0.0001	0.539 ± 0.048	0.369 ± 0.036	0.092 ± 0.016	1.46 ± 0.25
0.001 15 ± 0.000 05	0.494 ± 0.066	0.291 ± 0.050	0.215 ± 0.049	1.70 ± 0.38

Measurements at gas densities higher than 8% of LHD were not possible due to the high x-ray absorption in the very thick windows which would be required by such high gas pressures.

Although our measurements indicate that Coulomb deexcitation plays a significant role during the muonic cascade an unambiguous decision on the correct value of the scaling factor k is not yet possible. Moreover, the expected linear density dependence of K_α/K_β may be in doubt. The deviation from theory could also be an indication for more complex collisional processes, e.g., the existence of possible molecular effects [45]. A new experiment at very low gas densities [46] will also help to clarify the role of Coulomb deexcitation.

Financial support by the Austrian Science Foundation, the Austrian Academy of Sciences, the Swiss Academy of Sciences, the Swiss National Science Foundation, and the German Federal Ministry of Research and Technology is gratefully acknowledged. It is a pleasure to thank D. Sigg for his software support and D. Varidel for his excellent technical assistance. Fruitful discussions with E. C. Aschenauer and V. E. Markushin are acknowledged.

*Electronic address: lauss@amuon.imep.univie.ac.at
†Present address: University of California and L. Berkeley National Laboratory, Berkeley, CA 94720.

[1] M. Leon and H. A. Bethe, Phys. Rev. **127**, 636 (1962).
[2] J. S. Cohen, R. L. Martin, and W. R. Wadt, Phys. Rev. A **27**, 1821 (1983).
[3] G. A. Fesenko and G. Ya. Korenman, Hyperfine Interact. **101/102**, 91 (1996).
[4] D. Taqqu *et al.*, Hyperfine Interact. **101/102**, 599 (1996).
[5] M. Leon, Phys. Lett. **35B**, 413 (1971).
[6] V. E. Markushin, Zh. Eksp. Teor. Fiz. **80**, 35 (1981) [Sov. Phys. JETP **53**, 60 (1981)].
[7] V. E. Markushin, Phys. Rev. A **50**, 1137 (1994).
[8] E. C. Aschenauer and V. E. Markushin, Hyperfine Interact. **101/102**, 97 (1996); Z. Phys. D **39**, 165 (1997).
[9] Liquid Hydrogen Density (LHD) = 4.25 x 10^{22} atoms/cm^3.
[10] E. Borie and M. Leon, Phys. Rev. A **21**, 1460 (1980).
[11] F. Kottmann, in *Muonic Atoms and Molecules*, edited by L. A. Schaller and C. Petitjean (Birkhäuser, Basel, 1993), p. 219.
[12] L. Bracci and G. Fiorentini, Nuovo Cimento **43a**, 9 (1978).
[13] L. I. Men'shikov, Muon. Catal. Fusion **2**, 173 (1988).
[14] A. V. Kravtsov and A. I. Mikhailov, Zh. Eksp. Teor. Fiz. **107**, 1473 (1995) [Sov. Phys. JETP **80**, 822 (1995)]; Nukleonika **40**, 25 (1995).
[15] W. Czaplinski *et al.*, Phys. Rev. A **50**, 525 (1995).
[16] L. I. Ponomarev and E. V. Solov'ev, JETP Lett. **64**, 135 (1996).
[17] W. H. Breunlich, P. Kammel, J. S. Cohen, and M. Leon, Annu. Rev. Nucl. Part. Sci. **39**, 311 (1989).
[18] J. Zmeskal *et al.*, Phys. Rev. A **42**, 1165 (1990).
[19] P. Kammel, Lett. Nuovo Cimento **43**, 349 (1985).
[20] B. Lauss *et al.*, Phys. Rev. Lett. **76**, 4693 (1996).
[21] B. Lauss *et al.*, Hyperfine Interact. **101/102**, 285 (1996).
[22] B. Gartner *et al.*, Hyperfine Interact. **101/102**, 249 (1996).
[23] D. J. Abbot *et al.*, Phys. Rev. A **55**, 214 (1997).
[24] W. H. Breunlich, Nucl. Phys. **A335**, 137 (1980).
[25] W. H. Breunlich, Nucl. Phys. **A353**, 201c (1981).
[26] T. P. Terada and R. S. Hayano, Phys. Rev. C **55**, 73 (1997).
[27] A. Badertscher *et al.*, Phys. Lett. B **392**, 278 (1997).
[28] E. C. Aschenauer *et al.*, Phys. Rev. A **51**, 1965 (1995).
[29] D. Chatellard *et al.*, Phys. Rev. Lett. **74**, 4157 (1995).
[30] D. Sigg *et al.*, Phys. Rev. Lett. **75**, 3245 (1995).
[31] A. Placci *et al.*, Phys. Lett. **32B**, 413 (1970).
[32] B. Budick *et al.*, Phys. Lett. **34B**, 539 (1971).
[33] H. Anderhub *et al.*, Phys. Lett. **71B**, 443 (1977).
[34] P. O. Egan *et al.*, Phys. Rev. A **23**, 1152 (1981).
[35] H. Anderhub *et al.*, Phys. Lett. **143B**, 65 (1984).
[36] B. Lauss, Ph.D. thesis, University of Vienna 1997 (to be published).
[37] S. S. Gershtein, Zh. Eksp. Teor. Fiz. **43**, 706 (1962) [Sov. Phys. JETP **16**, 501 (1963)].
[38] B. Gartner, Diploma thesis, University of Graz, 1994.
[39] D. Varidel *et al.*, Nucl. Instrum. Methods Phys. Res., Sect. A **292**, 141 (1990).
[40] G. Fiorucci *et al.*, Nucl. Instrum. Methods Phys. Res., Sect. A **292**, 147 (1990).
[41] Type CCD-05-20-1-207 by EEV (English Electric Valve), Waterhouse Lane, Chelmsford, Essex, England.
[42] J.-P. Egger, D. Chatellard, and E. Jeannet, in *Muonic Atoms and Molecules* (Ref. [11]), p. 331.
[43] J.-P. Egger, D. Chatellard, and E. Jeannet, Part. World **3**, 139 (1993).
[44] D. Sigg, Nucl. Instrum. Methods Phys. Res., Sect. A **345**, 107 (1994).
[45] P. Froelich and J. Wallenius, Phys. Rev. Lett. **75**, 2108 (1995).
[46] F. J. Hartmann *et al.*, Hyperfine Interact. **101/102**, 623 (1996).